



ELSEVIER

Microelectronics Journal 35 (2004) 167–171

Microelectronics
Journal

www.elsevier.com/locate/mejo

On the simulation of the formation and dissolution of silicon self-interstitial clusters and the corresponding inverse modeling problem

Clemens Heitzinger*, Siegfried Selberherr

Institute for Microelectronics, Technical University of Vienna, Gusshausstrasse 27-29/E360, A-1040 Vienna, Austria

Received 15 September 2002; revised 25 March 2003; accepted 26 September 2003

Abstract

The formation and dissolution of silicon self-interstitial clusters is linked to the phenomenon of transient-enhanced diffusion (TED) which in turn has gained importance in the manufacturing of semiconductor devices. Based on theoretical considerations and measurements of the number of self-interstitial clusters during a thermal step, a model for the formation and dissolution of self-interstitial clusters is presented including the adjusted model parameters for two different technologies (i.e. material parameter sets). In order to automate the inverse modeling part, a general optimization framework was used. In addition to solving this problem, the same setup can solve a wide range of inverse modeling problems occurring in the domain of process simulation. Finally, the results are discussed and compared with a previous model.

© 2003 Elsevier Ltd. All rights reserved.

Keywords: Silicon self-interstitial clusters; Diffusion processes; Inverse problems

1. Introduction

The purpose of this work is to find a calibrated model for the formation and dissolution of silicon self-interstitial clusters of {311} defects. A good calibrated model for self-interstitial clustering is important for accurately simulating the transient-enhanced diffusion (TED) of impurities. TED is the fast displacement of impurities in the first thermal step just after implantation and the simulation of its evolution and magnitude is important in the manufacturing processes of submicron devices [1–3].

During initial annealing, implanted phosphorus and boron dopants in silicon show TED, since silicon interstitials are emitted from the region of implant damage. The structural source of these interstitials was unknown until a few years ago. In Ref. [4], the source of the silicon self-interstitials was shown to be the {311} defects which—as is generally agreed—consist of condensates of interstitials forming five- and seven-membered rings and can also be described in terms of one monolayer of hexagonal silicon [5]. These defects form rod-like structures along $\langle 110 \rangle$

directions and emerge from interstitials precipitating on {311} planes as a single monolayer of hexagonal silicon. From these defects, interstitials are emitted and give rise to TED, which was demonstrated using quantitative transmission electron microscopy measurements. In Ref. [4], the authors found a correlation between the evaporation of {311} defects during annealing at 670 and 815 °C and the length of the diffusion transient. Then they showed that the number of interstitials emitted by the defects is linked to the flux of interstitials driving TED and even suffices to explain the whole observed transient.

The interplay between the excess interstitials trapped in {311} defects and the boron concentration was discussed in Ref. [6] based on plan-view transmission electron microscopy. Furthermore, the implications of these results for TED were discussed and found to be important.

Counting the amount of self-interstitials is a non-trivial task, from transmission electron micrographs, the number of interstitials in each defect and thus the total number has to be measured. In Ref. [7], one can find measurements giving the number of interstitials as a function of time for annealing at four temperatures (670, 705, 738, and 815 °C) and $5 \times 10^{13} \text{ cm}^{-2}$, 40 keV boron implants. These measurements are shown in detail in Fig. 1 and provided the basis for the inverse modeling problem. For the computations, we

* Corresponding author. Tel.: +43-1-58801-36035; fax: +43-1-58801-36099.

E-mail address: heitzinger@iue.tuwien.ac.at (C. Heitzinger).

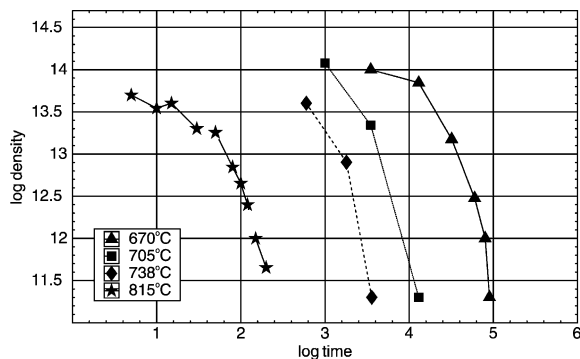


Fig. 1. The silicon self-interstitial density (in cm^{-3}) as a function of time (in s) for different annealing temperatures (interstitials stored in {113} or {311} defects after $5 \times 10^{13} \text{ cm}^{-2}$, 40 keV implants).

used TSUPREM-4 [8] and the optimization framework SIESTA [9,10].

We were interested in finding solutions for two different technologies corresponding to different sets of material parameters and hence different values for some TSUPREM-4 variables. In the following, we will call these parameter sets the high and the low parameter set (the latter being the TSUPREM-4 default values). The parameters and their values are shown in Table 1.

The model used contains several proposed models (e.g. Ref. [3]) as special cases [8]. After describing the model and the details of the inverse modeling problem, we present the results and our calibrated model parameters.

Table 1
The differences between the high and low (defaults) parameter set

TSUPREM-4 variable	High set	Low set
Pre-exponential constant for equilibrium concentration of interstitials (cm^{-3})	2.9×10^{24}	1.25×10^{29}
Activation energy for equilibrium concentration of interstitials (eV)	3.18	3.26
Pre-exponential constant for bulk recombination rate ($\text{cm}^3 \text{ s}^{-1}$)	1.2×10^{-5}	1.0×10^{-21}
Activation energy for bulk recombination rate (eV)	1.77	-1.0
Pre-exponential constant for surface recombination velocity at Si/oxide interface (cm s^{-1})	5.1×10^7	1.4×10^{-6}
Activation energy for surface recombination velocity at Si/oxide interface (eV)	1.77	-1.75
Pre-exponential constant for the diffusivity of vacancies ($\text{cm}^2 \text{ s}^{-1}$)	3.0×10^{-2}	3.65×10^{-4}
Activation energy for the diffusivity of vacancies (eV)	1.8	1.58
Pre-exponential constant for equilibrium concentration of vacancies (cm^{-3})	1.4×10^{23}	1.25×10^{29}
Activation energy for equilibrium concentration of vacancies (eV)	2.0	3.26

2. Modeling silicon self-interstitial cluster formation and dissolution

In Ref. [3], the following equation describing interstitial cluster kinetics is given

$$\frac{\partial C}{\partial t} = 4\pi\alpha a D_1 I C - \frac{C D_1}{a^2} e^{-E_b/kT}, \quad (1)$$

where $D_1 = D_0 e^{-E_m/kT}$ is the interstitial diffusivity, a is the average interatomic spacing, α is the capture radius expressed in units of a , $C(t, x)$ is the concentration of interstitials trapped in clusters, $I(t, x)$ is the concentration of free interstitials and T is the annealing temperature.

Here the main formula of the model for the change of the concentration of clustered interstitials is

$$\frac{\partial C}{\partial t} = K_{fi} \frac{I^{ifi}}{I_*^{isfi}} + K_{fc} \frac{I^{ifc}}{I_*^{isfc}} (C + \alpha I)^{cf} - K_r C^{cr}, \quad (2)$$

where $C(t, x)$ denotes the concentration of clustered interstitials, t time, $I(t, x)$ the concentration of unclustered interstitials, and $I_*(t, x)$ the equilibrium concentration of interstitials, which can be found by solving $\partial C(t, x)/\partial t = 0$. There are a number of parameters to be adjusted: K_{fi} , K_{fc} , K_r (the reaction constants); the exponents I^{ifi} , I^{isfi} , I^{ifc} , and I^{isfc} , cf , and cr ; and finally α .

The reaction constants are in the form of an Arrhenius expression, namely

$$K_{fi} = k_{fi} 0 e^{-k_{fi} E/kT},$$

$$K_{fc} = k_{fc} 0 e^{-k_{fc} E/kT},$$

$$K_r = k_r 0 e^{-k_r E/kT},$$

with the activation energies $k_{fi} 0 > 0$, $k_{fc} 0 > 0$, and $k_r 0 > 0$. Here T is the temperature (in Kelvin) and $k = 8.617 \times 10^{-5} \text{ eV K}^{-1}$, the Boltzmann constant. Since the coefficients $k_{fi} 0$, $k_{fc} 0$, and $k_r 0$ are positive, the first two terms in Eq. (2) are responsible for the formation of clusters and the last term for the dissolution. The sum of interstitials counted in C and I remains constant and the initial value of C is 10^9 cm^{-3} .

The terms I^{ifi}/I_*^{isfi} and I^{ifc}/I_*^{isfc} resemble the interstitial supersaturation, which is an approximation to the enhancement in diffusivity of interstitial diffusers such as boron or phosphorus and it can be deduced as follows. The solution I_e of $\partial C/\partial t = 0$ is often called the interstitial level. Then the interstitial supersaturation is the ratio of I_e to the equilibrium concentration I^* .

The first term $K_{fi} (I^{ifi}/I_*^{isfi})$ in Eq. (2) describes the joining of two clusters and thus, the expected values for the exponents are $ifi = 2 = isfi$. The second growth term

$$K_{fc} \frac{I^{ifc}}{I_*^{isfc}} (C + \alpha I)^{cf}$$

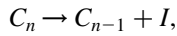
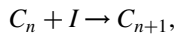
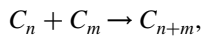
governs the case when an unclustered interstitial joins an interstitial cluster. Here, one can expect the exponents to be

unity. The second factor is a linear combination of C and I with an exponent.

Comparing Eqs. (1) and (2), the growth term of Eq. (1), basically being a reaction constant times IC , is split into two parts providing greater flexibility: one depending on a modified interstitial supersaturation term and one depending on a modified interstitial supersaturation term times $(C + \alpha I)^{cf}$.

The third term in Eq. (2) is the dissolution term in which—compared to Eq. (1)—an exponent was added.

To view Eq. (2) a bit differently, the reactions described in that equation can be obtained from the three basic reactions



where C_n is a cluster with n elements and I a sole interstitial.

3. Simulation setup, inverse modeling and results

In this section, the setup of the simulations, the inverse modeling problem, and its results are described. TSUPREM-4 was chosen for performing the simulations since it provides all the models necessary for the inverse modeling task.

Concerning the point defect modeling, a full, transient simulation of the two-dimensional point defect distributions was performed including the generation of point defects at interfaces, the diffusion of point defects into the substrate, the recombination at interfaces and in bulk silicon, the effects of dopant diffusion on the point defect concentration, the effects of pair saturation, and dopant-assisted recombination effects. Furthermore, oxidation-enhanced diffusion and high concentration effects were taken into account.

In the first simulation step, a 2 nm thick oxide was placed on the silicon surface, and the second step was a 5×10^9 atoms/cm², 40 keV implant. These first two steps were identical for all simulations. Then diffusion steps were performed corresponding to the time intervals and temperatures indicated in Fig. 1, where the self-interstitial concentration was recorded after each time step.

Two points from the measurements in Ref. [7] for 670 °C and one point for 705 °C were ignored since they were above the implanted dose. All measurements were viewed as one vector m . Let s be the vector of simulation results depending on the parameters p to be identified. The objective function $f(p)$ to be minimized was the quadratic mean of the element-wise relative error between a simulated point and a measured point, i.e.

$$f(p) := \sqrt{\frac{1}{n} \sum_{k=1}^n \left(\frac{s_k(p) - m_k}{m_k} \right)^2}.$$

Table 2

Variables, their intervals, and their units. $d0$ and dE are material parameters as described in the text, whereas the other variables are model parameters

Variable	Interval
$d0$ (cm ² s ⁻¹)	[25, 1000]
dE (eV)	[1.4, 1.85]
$kfi0$ (cm ^{-3(1 + isfi - ifi)} s ⁻¹)	[10 ²⁰ , 10 ²⁸]
$kfiE$ (eV)	[3.4, 6.0]
ifi	Constant = 2
isfi	Constant = 2
$kfc0$ (cm ^{-3(1 + isfc - ifc - cf)} s ⁻¹)	[10 ¹⁷ , 7 × 10 ¹⁹]
$kfcE$ (eV)	[4.9, 5.2]
ifc	Constant = 1
isfc	Constant = 1
α	[0, 5000]
cf	Constant = 1
$kr0$ (cm ^{-3(1 - cr)} s ⁻¹)	[1.5 × 10 ¹⁶ , 10 ¹⁸]
krE (eV)	[3.0, 3.62]
cr	Constant = 1

The variables of the objective function $f(p)$ are shown in Table 2. The variables $d0$ and dE determine the diffusivity $d0 e^{-dE/kT}$ of interstitials in silicon.

In order to reduce the time needed for the inverse modeling task, the optimization framework SIESTA was used. Its main tasks are optimizing a given objective function and parallelizing the executions of the objective function, which usually entails calling simulation tools in a loosely connected cluster of workstations. SIESTA provides several local and global optimizers, the ability to define complicated objective functions, and finally an interface to mathematica for examining the results. Fig. 2 shows an overview.

The optimization approach was to first identify reasonable ranges for the variables with great influence, namely energies and exponents. While identifying these ranges, suitable starting points for gradient-based optimization were found as well. Using these ranges and starting points, the optimizations proceeded automatically including all variables.

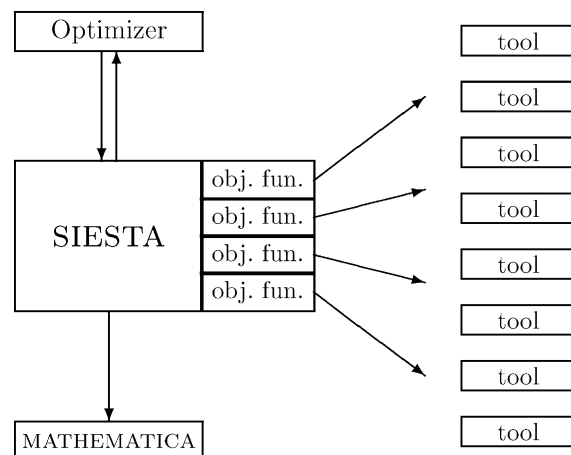


Fig. 2. Overview of SIESTA.

Table 3

Results for the high and low parameter sets with the above free variables. The mean relative error found is 0.389666 for the high parameter set and 0.504462 for the low parameter set

Free variable	Best point found
<i>High parameter set (mean relative error 0.389666)</i>	
d_0	51.7282
dE	1.76996
k_{fi0}	4.97576×10^{24}
k_{fiE}	3.77408
k_{fc0}	4.36789×10^{19}
k_{fcE}	4.95
α	1099.63
kr_0	2.77935×10^{16}
krE	3.56997
<i>Low parameter set (mean relative error 0.504462)</i>	
k_{fi0}	1.14156×10^{25}
k_{fiE}	3.94079
k_{fc0}	1.5051×10^{19}
k_{fcE}	5.81858
α	1563.1
cf	1.01287
kr_0	1.06467×10^{17}
krE	3.84503
cr	0.9639

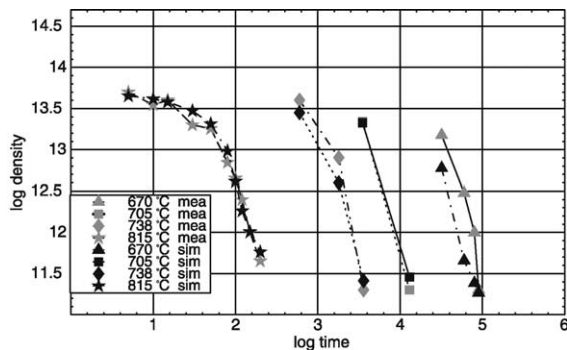


Fig. 3. Result for the high parameter set corresponding to parameter values shown in Table 3. The logarithm (base 10) of the simulated and measured concentration (cm^{-3}) of interstitial clusters is shown depending on time (s).

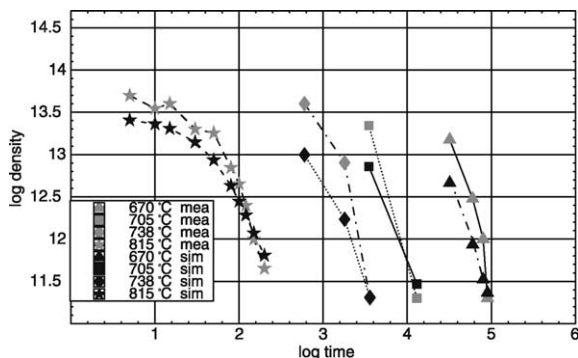


Fig. 4. Result for the low parameter set corresponding to parameter values shown in Table 3. The logarithm (base 10) of the simulated and measured concentration (cm^{-3}) of interstitial clusters is shown depending on time (s).

It was soon found that changing cf and cr did not yield improvements and whenever these variables could be used by a gradient-based optimizer, values very close to 1 resulted. The results described in Table 3 and Fig. 3 were obtained for the high parameter set.

Similarly, we carried out the same computations for the low parameter set, i.e. TSUPREM-4's default values. These results are shown in Table 3 and Fig. 4.

4. Conclusion

Starting with Eq. (2) and the measurements from Ref. [7], we adjusted a model for the formation and dissolution of silicon self-interstitial clusters, namely

$$\frac{\partial C}{\partial t} = K_{fi} \frac{I^2}{I_*^2} + K_{fc} \frac{I}{I_*} (C + \alpha I) - K_r C,$$

with values from Table 3. Although different values were also examined, the exponents in the first term were found to be equal to 2 ($ifi = 2 = isfi$), because two isolated interstitials can form a new cluster. Good results were achieved with $cf = 1$ and $ifc = 1 = isfc$, which means the rate of free interstitials joining already existing clusters depends linearly on the number of excess interstitials (interstitials above the equilibrium concentration) and a linear combination of the number of clusters and interstitials. Finally the exponent cr was found to be 1. This means that the rate of dissolution depends on the concentration of clustered interstitials and on the factor K_r .

The terms responsible for cluster formation in both models do not share a common structure, thus, we finally compare the results for the dissolution term. In Eq. (1), the dissolution term is

$$- \frac{D_0 C}{a^2} e^{-(E_b + E_m)/kT},$$

where the values for E_b and E_m given in Ref. [3] are 1.8 and 1.77 eV, respectively. $E_b + E_m = 3.57$ eV agrees very well with the values found for krE in Table 3, namely 3.56997 eV for the high parameter set and 3.84503 eV for the low parameter set.

In summary, a refined model for the formation and dissolution of silicon self-interstitial clusters was calibrated to published measurements for two different technologies (corresponding to two different sets of material parameters) and very good agreement was achieved. The inverse modeling problem was solved using an optimization framework providing several optimizers. Taking advantage of this automation, some variants of the models were investigated in order to challenge and verify theoretical considerations.

Acknowledgements

The authors acknowledge support from the ‘Christian Doppler Forschungsgesellschaft’, Vienna, Austria. They would also like to acknowledge the contributions of M. Kimura and M. Matsumura (Sony Hon-Atsugi Technology Center, Hon-Atsugi, Tokyo, Japan), who originally posed the problem.

References

- [1] C. Rafferty, H.-H. Vuong, S. Eshraghi, M. Giles, M. Pinto, S. Hillenius, Explanation of reverse short channel effect by defect gradients, in: Proceedings of the International Electron Devices Meeting, 1993, pp. 311–314.
- [2] C. King, R. Johnson, M. Pinto, H. Luftman, J. Munanka, In situ arsenic-doped polycrystalline silicon as a low thermal budget emitter contact for $\text{Si/Si}_{1-x}\text{Ge}_x$ heterojunction bipolar transistors, *Appl. Phys. Lett.* 68 (2) (1996) 226–228.
- [3] C. Rafferty, G. Gilmer, J. Jaraiz, D. Eaglesham, H.-J. Gossmann, Simulation of cluster evaporation and transient enhanced diffusion in silicon, *Appl. Phys. Lett.* 68 (17) (1996) 2395–2397.
- [4] D. Eaglesham, P. Stolk, H. Gossmann, J. Poate, Implantation and transient B diffusion in Si: the source of interstitials, *Appl. Phys. Lett.* 65 (18) (1994) 2305–2307.
- [5] S. Takeda, M. Kohyama, Structure refinement of the atomic model of the {113} defect in Si, in: American Institute of Physics Conference Series, vol. 134, 1993, pp. 33–36.
- [6] T. Haynes, D. Eaglesham, P. Stolk, H.-J. Gossmann, D. Jacobson, J. Poate, Interactions of ion-implantation-induced interstitials with boron at high concentrations in silicon, *Appl. Phys. Lett.* 69 (10) (1996) 1376–1378.
- [7] J. Poate, D. Eaglesham, G. Gilmer, J.-J. Gossmann, M. Jaraiz, C. Rafferty, P. Stolk, Ion implantation and transient enhanced diffusion, in: Proceedings of the International Electron Devices Meeting, Washington, DC, USA, 1995, pp. 77–80.
- [8] Avant! Corporation, TCAD Business Unit, Fremont, California, USA, TSUPREM-4, Two-Dimensional Process Simulation Program, Version 2000.2 User’s Manual, February 2000.
- [9] C. Heitzinger, S. Selberherr, An extensible TCAD optimization framework combining gradient based and genetic optimizers, in: Proceedings of the SPIE International Symposium on Microelectronics and Assembly: Design, Modeling, and Simulation in Microelectronics, Singapore, 2000, pp. 279–289.
- [10] R. Strasser, Rigorous TCAD investigations on semiconductor fabrication technology. Dissertation, Technische Universität Wien, <http://www.iue.tuwien.ac.at/phd/strasser>, 1999.